

# Self-consistent calculations of the optical properties of GaN quantum dots

V. Ranjan,\* G. Allan, C. Priester, and C. Delerue<sup>†</sup>

*Institut d'Electronique, de Microélectronique et de Nanotechnologie, département ISEN, UMR CNRS 8520,  
41 boulevard Vauban, Lille Cedex, France*

(Received 18 April 2003; revised manuscript received 7 July 2003; published 11 September 2003)

We present calculations of the transition energies and radiative lifetimes in GaN quantum dots embedded in AlN. The effects of elastic strains, and piezoelectric and pyroelectric fields are included. The electronic structure is described using a tight-binding method which takes into account the screening of the internal electric field by excited carriers in a fully self-consistent procedure. We show that the presence of one electron-hole pair in a quantum dot increases the optical gap by a few tens of meV and decreases significantly the radiative lifetime, which could give rise to very interesting nonlinear optical effects.

DOI: 10.1103/PhysRevB.68.115305

PACS number(s): 78.67.Hc, 73.22.-f

## I. INTRODUCTION

The fabrication of light emitters from the blue to the ultraviolet remains a challenge. In this context, group-III nitride compounds in general and GaN in particular have emerged as materials of choice,<sup>1</sup> not only for lasers<sup>2,3</sup> but also for other types of optical applications.<sup>4</sup> Recently, interest has grown to fabricate group-III nitride quantum wells and quantum dots, in particular because their light emission may cover a wide range of frequencies, from the red to the ultraviolet.<sup>5-12</sup> These structures reveal original properties due to the presence of strong internal pyroelectric and piezoelectric fields, mainly along the (0001) axis and in the range of a few MV/cm.<sup>13,14</sup> These fields are evidenced by the following observations:

(1) In large quantum wells<sup>5,6</sup> and quantum dots,<sup>8,15,16</sup> the photoluminescence energy is lower than the free exciton of GaN (Stark effect).

(2) The decay times of the photoluminescence exponentially decrease with emission energy, from tens of microseconds for systems emitting red light to nanoseconds for systems emitting ultraviolet light.<sup>10</sup> The reason is that the holes and the electrons are spatially separated by the internal fields, and therefore the overlap between electron and hole wave functions becomes negligible at large sizes, increasing the recombination time.<sup>8,10</sup>

(3) A significant blueshift is observed in GaN quantum dots as the excitation intensity is increased<sup>8</sup> because photo-created electrons and holes screen the internal fields. For this reason, large optical nonlinearities are expected in the systems.

On the theoretical side, the prediction of the optical properties of GaN quantum dots is complex because it must include the calculation of strains, confinement effects, and piezoelectric fields in structures containing a large number of atoms (typically  $10^4$ – $10^5$ ). In addition, the description of the screening by free carriers is only possible with self-consistent calculations. Thus, GaN quantum dots provide a major challenge for the theory. Recently, Andreev *et al.* have performed extensive calculations for pyramidal GaN quantum dots using a  $\mathbf{k}\cdot\mathbf{p}$  model in the envelope function approximation.<sup>17</sup> They further calculated the lifetime of the electron-hole pair.<sup>18</sup> In their calculation, they have generally

attained the trends observed in experiments. However, the screening of the electric fields was not considered, and thus nonlinear optical properties could not be studied.

In this paper we calculate the optical properties of GaN quantum dots, including the effect of strains, built-in electric fields and screening by excited carriers. The strains are calculated using three-dimensional (3D) finite-difference technique in elasticity theory. To account for screening effects, we calculate the charges and fields in a fully self-consistent way. The electronic structure is described by a tight-binding  $sp^3$  Hamiltonian which, in contrast to  $\mathbf{k}\cdot\mathbf{p}$  model, provides a good description of the bulk band structure in a wide range of energies and in the full Brillouin zone. We find that the transition energies are in close agreement with experiments if the magnitude of the built-in field along the (0001) direction is reduced with respect to the predicted values, confirming the trends obtained for quantum wells.<sup>10</sup> We show that the screening by excitons is efficient and we calculate the screening energy per exciton versus size of the quantum dots. We find that the lateral distribution of the piezoelectric field has little effect on the band gap of the system and that a constant field along the axis of growth can reproduce the results in the whole range of sizes.

The paper is organized as follows. Section II is devoted to the calculation of strains and fields in the system. The tight binding scheme is described in Sec. III. In Sec. IV, we present the results of the calculations for the transition energies, the electron-hole lifetime and the effect of screening, and we compare with the available experimental data. We conclude in Sec. V.

## II. STRAIN CALCULATIONS

### A. Geometry of the system

We present results on quantum dots consisting of truncated hexagonal pyramids of GaN embedded in AlN and standing on a thin GaN wetting layer. The geometry has been chosen as close as possible to experiments.<sup>15,16</sup> The largest dot we have considered is shown in Fig. 1. Defining the height of the truncated pyramids by  $h$  (including two monolayers for the wetting layer), we assume that the lateral size of the hexagons at the base and at the top vary like  $d_b$

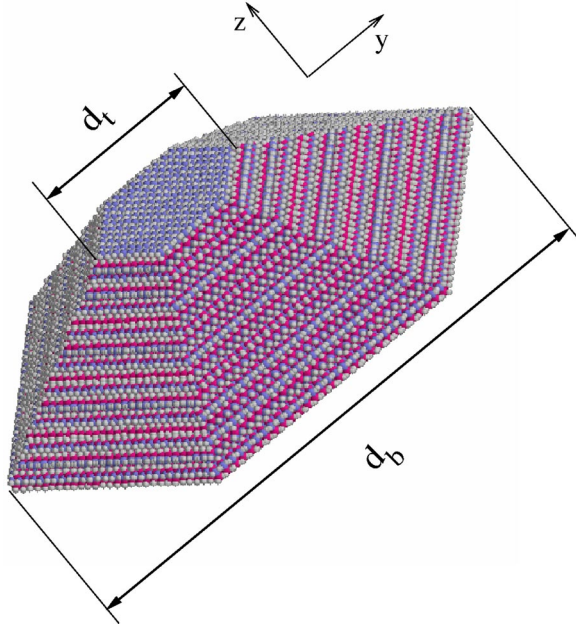


FIG. 1. (Color online) The largest cluster we have considered with about 40 000 Ga and N atoms. Its base size  $d_b$  is 17.7 nm, the height  $h$  is 4.3 nm, and the top size  $d_t$  is 5.0 nm. The height  $h$  includes two monolayers for the wetting layer. The bottom of the wetting layer is set at  $z=0$ .

$\approx 4.2h$  and  $d_t \approx d_b/3.5$ , respectively, which is justified by experimental data.<sup>16</sup> Quite similar rules have been used in the theoretical work of Ref. 17.

### B. Strains

To calculate the strains, we consider a square 2D array of truncated pyramidal quantum dots, and making use of continuum elasticity theory (finite elements method), we minimize the total elastic energy with respect to the strain components  $e_{ij}$ .<sup>19</sup> The strain elastic energy density in the crystallographic axis set is given by

$$\delta U = \frac{1}{2} \{ C_{11}(e_{xx}^2 + e_{yy}^2) + C_{33}e_{zz}^2 + 4C_{44}(e_{xz}^2 + e_{yz}^2) + 4C_{66}e_{xy}^2 + 2C_{12}e_{xx}e_{yy} + 2C_{13}(e_{xx}e_{zz} + e_{yy}e_{zz}) \}, \quad (1)$$

and the total elastic energy is obtained by integrating this energy density all over the finite element meshes. Basically, the results are extremely close to those of Andreev *et al.*,<sup>17</sup> the only difference being due to the fact that the system modeled in Ref. 17 corresponds to a 3D cubic array of quantum dots whereas we consider a 2D square array of quantum dots, which is closer to the experimental situation<sup>8,15,16</sup> where the dots were grown on a thick (1.5- $\mu\text{m}$ ) AlN buffer.

### C. Built-in fields

A particular property of group-III nitride heterostructures is the presence of large internal electric fields which arise from the spatial variations of the macroscopic polarization  $\mathbf{P}$ .

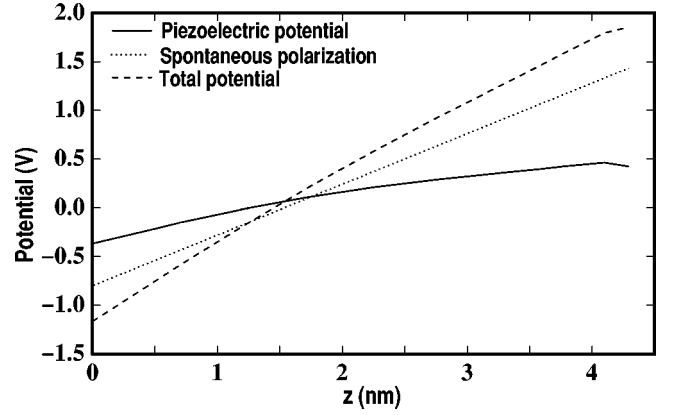


FIG. 2. The piezoelectric potential  $V_{\text{strain}}$ , the pyroelectric potential  $V_{\text{spont}}$ , and the total built-in potential  $V_b = V_{\text{spont}} + V_{\text{strain}}$  as a function of the position within the dot, along the (0001) direction ( $x=y=0$ ), through the center of the pyramid shown in Fig. 1.

Due to the wurtzite structure,  $\mathbf{P}$  has a nonzero contribution in absence of strain, the so-called spontaneous polarization  $\mathbf{P}_{\text{spont}}$ .<sup>20</sup> Elastic strains produce a variation of the polarization ( $\mathbf{P} = \mathbf{P}_{\text{spont}} + \mathbf{P}_{\text{strain}}$ ) which is determined by the piezoelectric constants.

To determine the pyroelectric field induced by the spontaneous polarization, we calculate the equivalent surface charge density  $\sigma_{\text{spont}}$  at the GaN/AlN interfaces as

$$\sigma_{\text{spont}} = \Delta \mathbf{P}_{\text{spont}} \cdot \mathbf{n}, \quad (2)$$

where  $\mathbf{n}$  is the unit vector normal to the interface and  $\Delta \mathbf{P}_{\text{spont}}$  is the discontinuity of the spontaneous polarization across the interface. The induced electrostatic potential  $V_{\text{spont}}$  is calculated by replacing the density  $\sigma_{\text{spont}}$  by point charges on each atom at the GaN/AlN interface. We have checked that this discretization has a negligible effect on the potential inside the dot.

The piezoelectric polarization field is nonuniform, and thus gives rise to a piezoelectric potential calculated as

$$V_{\text{strain}}(\mathbf{r}) = \frac{1}{4\pi\epsilon_0\epsilon_r} \int \frac{\mathbf{P}_{\text{strain}}(\mathbf{r}') \cdot (\mathbf{r} - \mathbf{r}')}{|\mathbf{r} - \mathbf{r}'|^3} d^3\mathbf{r}', \quad (3)$$

where  $\epsilon_0$  is the vacuum permittivity and  $\epsilon_r$  is the relative dielectric constant. We use  $\epsilon_r = 9.6$  in the whole structure, which is the range of the reported values for GaN and AlN.<sup>21–23</sup>

The total bare potential  $V_b = V_{\text{spont}} + V_{\text{strain}}$  is calculated using the values of Ref. 13 for the piezoelectric constants and spontaneous polarization, and using the values of Ref. 24 for the elastic constants. The main variation of the potential is along the  $z$  direction as shown in Fig. 2 for the quantum dot of Fig. 1. The magnitude of the electric field varies from  $\approx 8.5$  MV/cm at the base of the pyramid to  $\approx 6.2$  MV/cm at the top. These values are larger than those obtained in Ref. 17 ( $\approx 6$  MV/cm and  $\approx 4$  MV/cm, respectively). The difference comes from the fact that we consider a single 2D array of quantum dots, whereas in Ref. 17 the system is periodic in

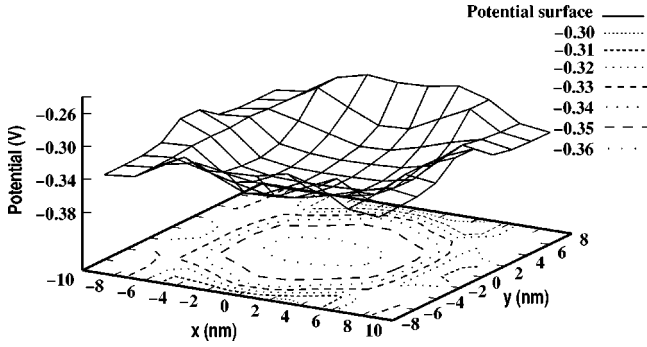


FIG. 3. Contour and surface plots of the piezoelectric potential  $V_{\text{strain}}$  in the  $x$ - $y$  plane ( $z=0$ ), for the quantum dot of Fig. 1. The electrostatic potential forms a bowl, which confines the holes towards the center of the dot.

the  $z$  direction. However, the trends in the variations of the potentials are similar in the two calculations.

Figure 3 shows the variations of the electrostatic potential in the  $x$ - $y$  plane due to the strain component. In agreement with Ref. 17, the resulting electric field is much smaller than in the  $z$  direction. It leads to a weak potential well for the holes towards the center of the pyramids.

### III. TIGHT-BINDING CALCULATIONS

We describe in this section the method to calculate the electronic structure of the quantum dots. Whereas *ab initio* approaches are limited to small systems ( $\approx 200$  atoms), tight-binding methods<sup>26,25</sup> allow to calculate the electronic states in a much wider range of sizes and thus can be directly connected to experiments. Recently, self-consistent tight binding calculations using a  $sp^3d^5s^*$  atomic basis have been applied to 2D GaN/InGaN structures,<sup>27</sup> and tight binding parameters have been developed for group-III nitride semiconductors.<sup>28,29</sup> But our calculations for 0D structures are computationally more demanding than for quantum well structures where Bloch's theorem can be applied in two directions. Thus we have used a  $sp^3$  basis to reduce the size of the Hamiltonian matrix. The parameters for GaN, including second-nearest-neighbor interactions (Table I), have been obtained by fitting the band structure and the effective masses obtained by calculations that we have performed in the local-density approximation<sup>31</sup> (the width of the band gap is adjusted on the experimental one to avoid the intrinsic band-gap problem of the local-density approximation, see Ref. 25). The band structure of GaN calculated in tight-binding case is shown in Fig. 4.

The description of the AlN barrier raises a difficulty. Published values for the valence-band discontinuity at the GaN/AlN interface are widely spread, between 0.5 eV and 1.4 eV.<sup>32-38</sup> Taking into account this uncertainty, the large band gap of AlN (6.2 eV), the fact that the hole mass in GaN is heavy (close to the free-electron mass), and that the total electric field creates deep potential wells for the electrons and holes,<sup>17</sup> we make the approximation of an infinite barrier for AlN. As a matter of fact, we use pseudohydrogen atoms and adjust the Ga-H and N-H tight-binding interactions in

TABLE I. Top: second nearest neighbor tight-binding parameters for GaN. The notation is that of Slater and Koster (Ref. 30)  $a$  represent-anion, and  $c$  represent-cation.  $\Delta$  is the spin-orbit coupling parameter. Bottom: effective masses for the conduction band (c), the heavy (hh), and light (lh) hole bands along the  $z$  axis ( $\parallel$ ) and along the transverse directions ( $\perp$ ) in units of the free-electron mass.

Tight-binding parameters for GaN (eV)			
$E_s^a$	-10.70425	$E_p^a$	-2.18636
$E_s^c$	6.47663	$E_p^c$	8.48538
$\Delta^a$	0.004	$\Delta^c$	0.0400
First nearest neighbor interactions (eV)			
$E_{ss\sigma}(ac)$	-1.79002	$E_{sp\sigma}(ca)$	2.64275
$E_{sp\sigma}(ac)$	3.13210	$E_{pp\pi}(ac)$	-1.58414
$E_{pp\sigma}(ac)$	1.35580		
Second-nearest-neighbor interactions (eV)			
$E_{ss\sigma}(aa)$	-0.21488	$E_{sp\sigma}(aa)$	-0.03594
$E_{pp\sigma}(aa)$	0.32853	$E_{pp\pi}(aa)$	0.17167
$E_{ss\sigma}(cc)$	-0.51133	$E_{sp\sigma}(cc)$	0.84729
$E_{pp\sigma}(cc)$	1.49551	$E_{pp\pi}(cc)$	-0.39783
Effective masses			
$m_{\parallel}^c$	0.193	$m_{\perp}^c$	0.189
$m_{\parallel}^{\text{hh}}$	1.288	$m_{\perp}^{\text{hh}}$	0.447
$m_{\parallel}^{\text{lh}}$	0.617	$m_{\perp}^{\text{lh}}$	0.281

order to push the surface states far from the band edges. As shown in Ref. 17 and in the following, this is not a severe approximation in the range of sizes measured experimentally because the electron and hole energies are mainly determined by the magnitude of the built-in electric field.

To illustrate the effect of the quantum confinement alone, and even if it is not in the main scope of the paper, we present in Fig. 5 the gap of spherical GaN nanocrystals as a function of size. These results may apply, for example, to nanocrystals embedded in a  $\text{SiO}_2$  oxide matrix or dispersed in a solvent.<sup>39</sup> The confinement energy is equal to 0.5 eV for a diameter of 2.9 nm, a quite small value compared to other semiconductors<sup>25,26</sup> where, for example, a shift of 0.5 eV is obtained for a 3.8-nm silicon nanocrystal.<sup>25</sup> These results are supported by photoluminescence experiments on GaN nanocrystals showing only a small blueshift for particle sizes

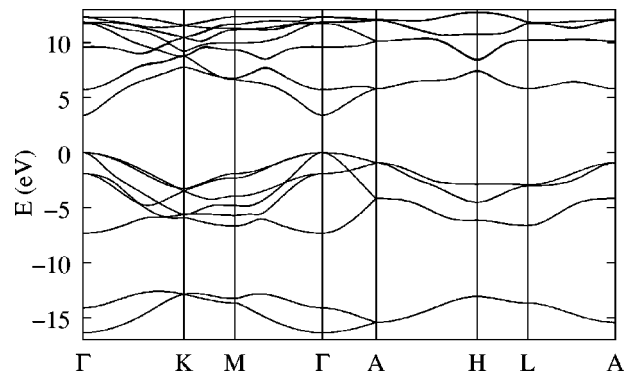


FIG. 4. Band structure of bulk GaN (hexagonal structure). The zero of energy corresponds to the top of the valence band.

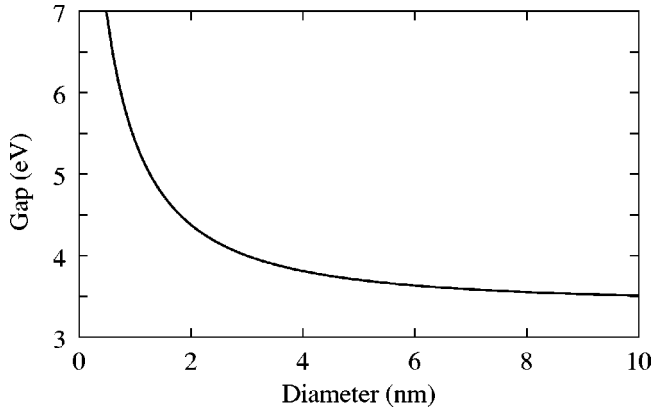


FIG. 5. Band gap as a function of size of spherical GaN nanocrystals. The bulk band gap is 3.5 eV.

of  $30 \pm 12 \text{ \AA}$  (Ref. 39) (there is probably no internal field in these nanocrystals because they have a zinc-blende structure.<sup>39</sup>)

The built-in potential  $V_b$  shown in Fig. 2 creates a potential well (i) at the bottom of the dot for holes and (ii) at the top of the dot for electrons. The charge distribution induced by the spatial separation of electrons and holes within the dot creates an electric field  $V_{scr}$  which tends to screen the bare field. To include this effect, we solve the Schrödinger and Poisson equations self-consistently, which correspond to the Hartree approximation.<sup>40</sup> The total potential  $V = V_b + V_{scr}$  is introduced into the tight-binding Schrödinger equation, the wave functions are calculated, the new charge distributions are derived, and the procedure is iterated up to self-consistency. Then we calculate the transition energies, i.e., the energies for exciting successively one electron-hole pair in the quantum dot. The transition energies are given by  $E(n+1, n+1) - E(n, n)$ , where  $E(n, p)$  is the total Hartree energy of the system with  $n$  electrons and  $p$  holes. They are calculated to a good degree of approximation by using Slat-

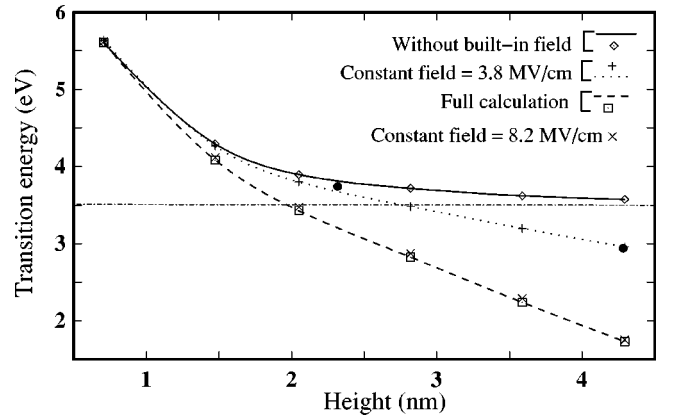


FIG. 6. Transition energy to excite one electron-hole pair from the ground state as a function of the height of pyramidal quantum dots and plotted in four cases: (i) without built-in field, (ii) self-consistent calculation including the piezoelectric field and the spontaneous polarization of Ref. 13, (iii) using a constant field of 8.2 MV/cm, and (iv) using a constant field of 3.8 MV/cm. The experimental data (●) are from Ref. 8. The horizontal dotted-dashed line corresponds to the bulk GaN band gap.

er's transition state,<sup>41</sup> expressing  $E(n+1, n+1) - E(n, n) = \epsilon_g(n+1/2, n+1/2)$ , the one-particle gap calculated self-consistently with an occupation of  $n+1/2$  electron and  $n+1/2$  hole.

#### IV. RESULTS AND DISCUSSIONS

Figure 6 shows the transition energy versus size for the first excitation [ $E(1,1) - E(0,0)$ ]. When the height of the pyramids exceeds 2 nm, the effect of the confinement alone is small, confirming the results obtained on spherical nanocrystals. Thus the optical gap is mainly determined by the magnitude of internal fields. In particular, the full calculation including piezoelectric and pyroelectric fields obtained with

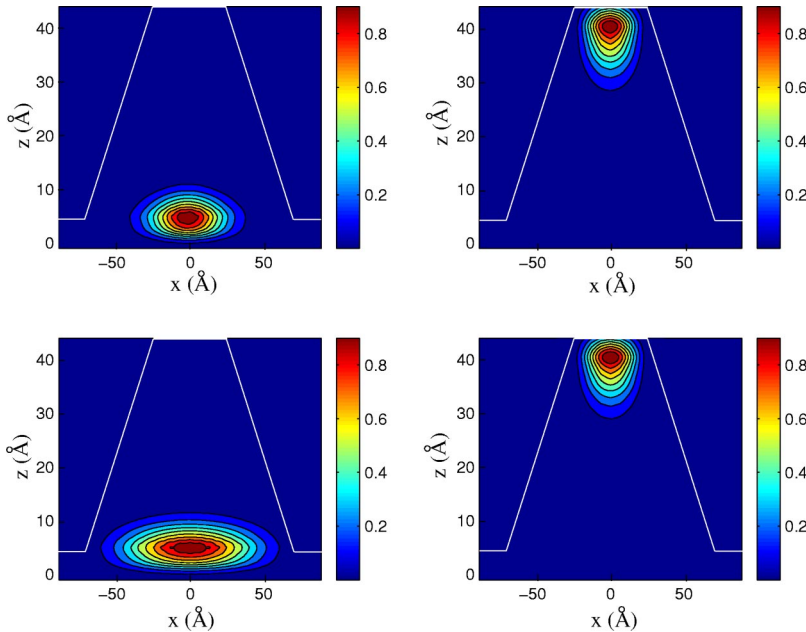


FIG. 7. (Color online) Charge densities for the electron (right side) and the hole (left) in the quantum dot of Fig. 1. The figures at the top are obtained by the full calculation including the spontaneous polarization and strains, showing that the hole is laterally confined when the piezoelectric field is taken into account. The figures at the bottom are obtained with a constant field of 8.2 MV/cm. For the clarity of the figures, the vertical and horizontal scales are not the same.



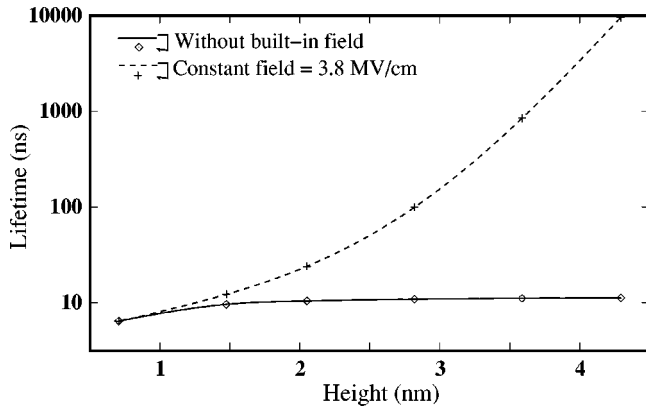


FIG. 8. Calculated radiative lifetime for the transition from the first excitonic state ( $n=p=1$ ) to the ground state ( $n=p=0$ ) as a function of the quantum dot height.

the parameters of Ref. 13 shows that the optical gap is below the bulk excitonic transition for heights above 2 nm. Interestingly, a constant field of 8.2 MV/cm can reproduce the results in the full range of sizes, confirming that the transition energies depend most strongly on the field along the (0001) axis.<sup>8,17</sup> Figure 6 also shows that a constant field of about 3.8 MV/cm fits well the experimental data of Ref. 8, while for 8.2 MV/cm the transition energies are too small at large sizes. We conclude that the field along the (0001) direction must be reduced compared to the value deduced with the piezoelectric constants and the spontaneous polarization predicted in Ref. 13. This is consistent with previous analysis of the optical properties of quantum wells.<sup>6,10,42,43</sup> Several reasons for this reduction have been invoked,<sup>10</sup> such as the neutralization of charges at the surfaces<sup>44</sup> or the presence of residual free carriers<sup>45,46</sup> which, in the case of quantum dots, would lead to charged excitons.

Figure 7 confirms that the hole wave function is localized at the bottom of the quantum dot, partly in the wetting layer, while the electron wave function is pushed up to the top. It also shows that the piezoelectric field induces an extra lateral confinement for the hole towards the center of the dot, in agreement with Ref. 17. Such a lateral confinement is clearly absent when one replaces the pyroelectric and piezoelectric fields by a constant field of 8.2 MV/cm along the (0001) direction. However, as shown above, the lateral confinement has no significant influence on the transition energies.

Figure 8 presents the dependence on emission energy of the radiative lifetime. When the built-in fields are not included in the calculation, there are no significant variations while, when the fields are introduced, the lifetime quickly increases with size, with an exponential law for large quantum dots. These results are in agreement with the theoretical work of Ref. 18.

Let us now discuss the effect of the screening by excited carriers. Figure 9 shows the evolution of the gap as a function of the number  $n$  of electron-hole pairs in the largest quantum dot that we have considered. The electron-hole pairs formed in the quantum dot screen the built-in field and hence lead to a blueshift of the transition energy. The variation of the gap with  $n$  is approximately linear. Recent calcu-

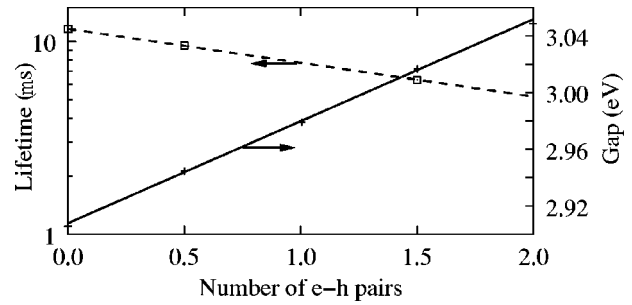


FIG. 9. Dependence of the one-particle gap and of the radiative lifetime on the number  $n$  of electron-hole pairs in the quantum dot of Fig. 1. A constant field of 3.8 MV/cm was considered in the calculations. The gap follows a linear law given by  $\epsilon_g = 2.927 + 0.063n$  (eV).

lations on InAs quantum dots submitted to an external electric field applied by a metallic tip also predict a linear variation of the gap with the number of injected carriers.<sup>40</sup> Figure 10 presents the evolution with size of the screening energy which we define as the variation in energy gap per electron-hole pair. We obtain a screening energy of 63 meV for the largest dot. Experimentally, a 70-meV blueshift is observed when the power density of the laser exciting the dots varies from 60 to 450 W/cm<sup>2</sup>.<sup>8</sup> A few electron-hole pairs per dot are estimated at the higher density. From our work, we conclude that a single pair can explain this blueshift. The screening energy decreases when going to small size because the overlap between the hole and electron wave functions increases due to a stronger confinement, which tends to reduce the screening field.

Below 1.5 nm, our calculations predict that the screening energy increases (Fig. 10). However, we must note that in this range of sizes where the electron-hole overlap is large, the Coulomb interaction between the two particles is not correctly described in the Hartree approximation. Thus, a two-particle calculation should be required in this limit, for example, by solving the Bethe-Salpeter equation.<sup>47</sup> With atomistic descriptions of the electronic structure, such as tight

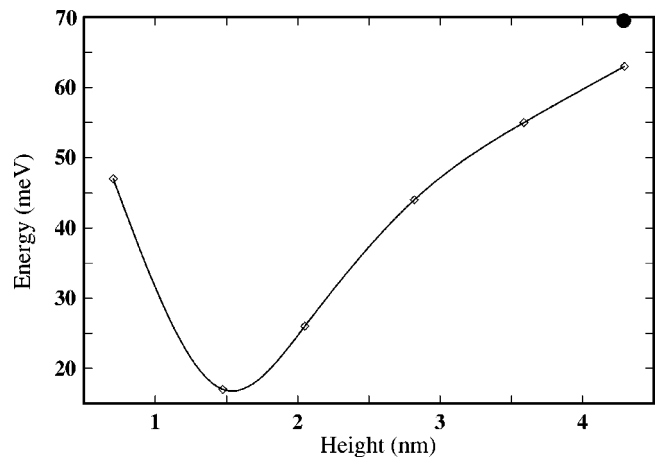


FIG. 10. Screening energy as a function of the quantum dot height. A constant field of 3.8 MV/cm was considered in the calculations. The experimental point (●) is from Ref. 8.

binding or empirical pseudopotentials, one possible approach would be to use a configuration-interaction technique like in Refs. 47–49. But, in addition, the procedure should be made self-consistent. This is beyond the scope of the present paper, and could be the purpose of future works.

Figure 9 shows that the radiative lifetime has an exponential dependence on the number  $n$  of excitations, which can be understood as follows. The screening field is a linear function of  $n$ , and the lifetime is an exponential function of the field through the overlap between the electron and hole wave functions. The variation of the lifetime is substantial, and thus should be experimentally measurable if nonradiative effects do not predominate.

## V. CONCLUSIONS

We have performed atomistic calculations for the electronic structure of GaN quantum dots containing up to approximately 40 000 atoms using second-nearest-neighbor

$sp^3$  tight-binding method. The piezoelectric field is taken into account through the calculation of strains and we also include the pyroelectric field. We use a self-consistent approach to describe the electron-hole charge separation resulting from the presence of the internal fields. We show that the addition of one electron-hole pair in a dot increases the gap by a few tens of meV, in good agreement with an earlier experimental observation. The nonlinear optical effects may play an important role in these systems due to the screening of internal fields, which may be particularly interesting for applications such as optical memories.<sup>50</sup>

## ACKNOWLEDGMENTS

This work has been supported by an “Action Concertée Incitative” of the French Ministry of Research and of the Centre National de la Recherche Scientifique. We would like to thank Pierre Lefebvre for suggesting us the problem and for helpful discussions.

\*Present address: Physics Department, University of Arkansas, Fayetteville, AR 72701; Electronic address: vranjan@uark.edu

†Electronic address: christophe.delerue@isen.fr

<sup>1</sup>S. Nakamura, *Semicond. Sci. Technol.* **14**, R27 (1999).

<sup>2</sup>F.A. Ponce and D.P. Bour, *Nature (London)* **386**, 351 (1997).

<sup>3</sup>N.M. Johnson, A.V. Nurmikko, and S.P. DenBaars, *Phys. Today* **53** (10), 31 (2000).

<sup>4</sup>C. Gmachl, M.Ng. Hock, S.N.G. Chu, and A.Y. Cho, *Appl. Phys. Lett.* **77**, 3722 (2000).

<sup>5</sup>N. Grandjean and J. Massies, *Appl. Phys. Lett.* **73**, 31 (1998).

<sup>6</sup>M. Leroux, N. Grandjean, M. Lügt, J. Massies, B. Gil, P. Lefebvre, and P. Bigenwald, *Phys. Rev. B* **58**, R13 371 (1998).

<sup>7</sup>B. Daudin, F. Widmann, J. Simon, G. Feuillet, J.L. Rouvière, N.T. Pelekanos, and G. Fishman, *MRS Internet J. Nitride Semicond. Res.* **4S1**, G9.2 (1999).

<sup>8</sup>F. Widmann, J. Simon, B. Daudin, G. Feuillet, J.L. Rouvière, N.T. Pelekanos, and G. Fishman, *Phys. Rev. B* **58**, R15 989 (1998).

<sup>9</sup>P. Lefebvre, T. Taliercio, A. Morel, J. Allègre, M. Gallart, B. Gil, H. Mathieu, B. Damilano, N. Grandjean, and J. Massies, *Appl. Phys. Lett.* **78**, 1538 (2001).

<sup>10</sup>T. Taliercio, P. Lefebvre, M. Gallart, and A. Morel, *J. Phys.: Condens. Matter* **13**, 7027 (2001).

<sup>11</sup>K. Tachibana, T. Someya, and Y. Arakawa, *Appl. Phys. Lett.* **74**, 383 (1999).

<sup>12</sup>B. Damilano, N. Grandjean, F. Semond, J. Massies, and M. Leroux, *Appl. Phys. Lett.* **75**, 962 (1999).

<sup>13</sup>F. Bernardini, V. Fiorentini, and D. Vanderbilt, *Phys. Rev. B* **56**, R10 024 (1997).

<sup>14</sup>F. Bechstedt, U. Grossner, and J. Furthmüller, *Phys. Rev. B* **62**, 8003 (2000).

<sup>15</sup>M. Arley, J.L. Rouvière, F. Widmann, B. Daudin, G. Feuillet, and H. Mariette, *Appl. Phys. Lett.* **74**, 3287 (1999).

<sup>16</sup>F. Widmann, B. Daudin, G. Feuillet, Y. Samson, J.L. Rouvière, and N.T. Pelekanos, *J. Appl. Phys.* **83**, 7618 (1998).

<sup>17</sup>A.D. Andreev and E.P. O’Reilly, *Phys. Rev. B* **62**, 15 851 (2000).

<sup>18</sup>A.D. Andreev and E.P. O’Reilly, *Appl. Phys. Lett.* **79**, 521 (2001).

<sup>19</sup>F. Lelarge, O. Dehaese, E. Kapon, C. Priester, *Appl. Phys. A: Mater. Sci. Process.* **69**, 347 (1999); Y.M. Niquet, C. Priester, C.

Gourgon, and H. Mariette, *Phys. Rev. B* **57**, 14 850 (1998).

<sup>20</sup>N. W. Ashcroft and N. D. Mermin, *Solid State Physics* (Harcourt Brace, New York, 1976).

<sup>21</sup>A.T. Collins, E.C. Lightowlers, and P.J. Dean, *Phys. Rev.* **158**, 833 (1967).

<sup>22</sup>Y. Goldberg, in *Properties of Advanced Semiconductor Materials GaN, AlN, InN, BN, SiC, SiGe*, edited by M. E. Levinshtein, S. L. Rumyantsev, and M. S. Shur (Wiley, New York, 2001), p. 31.

<sup>23</sup>V. Bougrov, M. E. Levinshtein, S. L. Rumyantsev, and A. Zubrilov, in *Properties of Advanced Semiconductor Materials GaN, AlN, InN, BN, SiC, SiGe*, edited by M. E. Levinshtein, S. L. Rumyantsev, and M. S. Shur (Wiley, New York, 2001), p. 1.

<sup>24</sup>A.F. Wright, *J. Appl. Phys.* **82**, 2833 (1997).

<sup>25</sup>Y.M. Niquet, C. Delerue, G. Allan, and M. Lannoo, *Phys. Rev. B* **62**, 5109 (2000).

<sup>26</sup>G. Allan, Y.M. Niquet, and C. Delerue, *Appl. Phys. Lett.* **77**, 639 (2000).

<sup>27</sup>F. Della Sala, A. Di Carlo, Paolo Lugli, F. Bernardini, V. Fiorentini, R. Scholz, and J.-M. Jancu, *Appl. Phys. Lett.* **74**, 2002 (1999).

<sup>28</sup>J.-M. Jancu, R. Scholz, F. Beltram, and F. Bassani, *Phys. Rev. B* **57**, 6493 (1998).

<sup>29</sup>J.-M. Jancu, F. Bassani, F. Della Sala, and R. Scholz, *Appl. Phys. Lett.* **81**, 4838 (2002).

<sup>30</sup>J.C. Slater and G.F. Koster, *Phys. Rev.* **94**, 1498 (1954).

<sup>31</sup>X. Gonze *et al.*, *Comput. Mater. Sci.* **25**, 478 (2002).

<sup>32</sup>J. Baur, K. Maier, M. Kunzer, U. Kaufmann, and J. Schneider, *Appl. Phys. Lett.* **65**, 2211 (1994).

<sup>33</sup>S.W. King, C. Ronning, R.F. Davis, M.C. Benjamin, and R.J. Nemanich, *J. Appl. Phys.* **84**, 2086 (1998).

<sup>34</sup>Z. Sitar, M.J. Paisley, B. Yabn, R.F. Davis, J. Ruan, and J.W. Choyke, *Thin Solid Films* **200**, 311 (1991).

<sup>35</sup>J.R. Waldrop and R.W. Grant, *Appl. Phys. Lett.* **68**, 2879 (1996).

<sup>36</sup>G. Martin, A. Botchkarev, A. Rockett, and H. Morkoc, *Appl. Phys. Lett.* **68**, 2541 (1996).

<sup>37</sup>F. Bernardini and V. Fiorentini, *Phys. Rev. B* **57**, R9427 (1998).

<sup>38</sup>M.B. Nardelli, K. Rapcewicz, and J. Bernholc, *Phys. Rev. B* **55**, R7323 (1997).

- <sup>39</sup>O.I. Mičić, S.P. Ahrenkiel, D. Betram, and A. Nozik, *Appl. Phys. Lett.* **75**, 478 (1999).
- <sup>40</sup>Y.M. Niquet, C. Delerue, G. Allan, and M. Lannoo, *Phys. Rev. B* **65**, 165334 (2002).
- <sup>41</sup>J. C. Slater, *Quantum Theory of Atomic Structure* (McGraw-Hill, New York, 1960).
- <sup>42</sup>N. Grandjean, B. Damilano, S. Dalmaso, M. Leroux, M. Laugt, and J. Massies, *J. Appl. Phys.* **86**, 3714 (1999).
- <sup>43</sup>J.A. Garrido, J.L. Sanchez-Rojas, A. Jimenez, E. Muñoz, F. Omnes, and P. Gibart, *Appl. Phys. Lett.* **75**, 2407 (1999).
- <sup>44</sup>J.P. Ibbetson, P.T. Fini, K.D. Ness, S.P. DenBaars, J.S. Speck, and U. Mishra, *Appl. Phys. Lett.* **77**, 250 (2000).
- <sup>45</sup>J.L. Sanchez-Rojas, J.A. Garrido, and E. Muñoz, *Phys. Rev. B* **61**, 2773 (2000).
- <sup>46</sup>O. Ambacher, B. Foutz, J. Smart, J.R. Shealy, N.G. Weimann, K. Chu, M. Murphy, A.J. Sierakowski, W.J. Schaff, L.F. Eastman, R. Dimitrov, A. Mitchell, and M. Stutzmann, *J. Appl. Phys.* **87**, 334 (2000).
- <sup>47</sup>C. Delerue, M. Lannoo, and G. Allan, *Phys. Rev. Lett.* **84**, 2457 (2000); **89**, 249901(E) (2002).
- <sup>48</sup>E. Martin, C. Delerue, G. Allan, and M. Lannoo, *Phys. Rev. B* **50**, 18 258 (1994).
- <sup>49</sup>A. Franceschetti, A. Williamson, and A. Zunger, *J. Phys. Chem.* **104**, 3398 (2000).
- <sup>50</sup>P. Lefebvre (private communication).